LNF-95/022

Simulation of the Electromagnetic component of Extensive Air Showers

V. Patera, M. Carboni, G. Battistoni, A. Ferrari

Nucl. Instr. & Meth. In Phys. Res. A 356, 514-525, (1995)

Nuclear Instruments and Methods in Physics Research A 356 (1995) 514–525

NUCLEAR INSTRUMENTS & METHODS IN PHYSICS RESEARCH Section A

ELSEVIER

Simulation of the electromagnetic component of extensive air showers

V. Patera [b,*], M. Carboni [a], G. Battistoni [c], A. Ferrari [c]

[a] *INFN-Laboratori Nazionali di Frascati, P.O. Box 13, I-00044 Frascati, Italy*
[b] *Dipartimento di Energetica, Facolta' di Ingegneria, dell' Universita' di Roma ''La Sapienza'', Italy*
[c] *INFN-Milano, via Celoria 16, I-20133 Milano, Italy*

Received 20 June 1994; revised form received 3 October 1994

Abstract

The e.m. component of extensive air showers, as sampled at a given atmospheric depth, may be considered as the superposition of sub-showers initiated by photons and electrons (positrons) mainly coming from the decay of secondary mesons. A detailed simulation of showers in atmosphere as produced by gammas and electrons has been performed by means of standard high energy physics Monte Carlo codes. We developed a set of parametrizations of these sub-showers to be included in the full simulations of extensive air showers with the aim to reduce the required computer power. Comparisons with previous results found in the literature are shown.

1. Introduction

The experiments measuring extensive air showers (EAS) nowadays have reached a high level of complexity and sizeable dimensions, producing a corresponding increase in the quality and statistics of the experimental data. The analysis of such high quality data needs adequate simulations of the shower development in the atmosphere and of the response of the detector.

The accurate simulation of a large number of EAS produced by primary nuclei with energy ranging up to 10^5 TeV and beyond [1] is a formidable task in terms of computing power. One the other hand most of the present cosmic ray shower generators [2] provide the opportunity to follow the secondary particles produced at different depths in the atmosphere (e.g. photons from π^0 decay, electrons from semileptonic decays of K, etc.). In order to maintain computer time within reasonable limits, these secondaries are followed down to a suitable, not too low, energy threshold. It is then assumed that each of these secondaries originates a sub-shower contributing to the total e.m. ''size'' measured by air shower arrays. The average number of electrons/positrons arriving at the depth of the shower array from each sub-shower is often derived from existing analytical shower approximations [3]. Fluctuations of individual sub-showers are usually neglected, due to the common belief that they are overwhelmed by the fluctuations in the development of the extensive air shower itself.

This work originates from the need to test the range of validity of these analytical approximations. Furthermore, a known limit of the quoted formulae is that they are constructed to give a number of equivalent charged particles, but real experiments, like those based on arrays of scintillators, are also sensitive to the conversion of gamma rays, which are known to dominate the shower development beyond the maximum. In a practical situation, if thick scintillator counters are used, a significant number of these photons will interact in the sensitive medium, contributing to the detected signal. This effect is also known as ''Transition effect'', after the work of Rossi and Greisen [4]. In the analysis of experimental data an estimated correction factor is usually inserted. Therefore it is useful to give expressions for the number of secondary electrons/positrons and gammas separately, together with their energy distributions. A detailed simulation of the number of electrons and positrons in air showers from different primaries can already be found in Ref. [10].

In this work we have used specialised shower programs commonly used in high energy physics to extract a set of parametrizations to describe the sub-showers initiated by secondary particles at different energies and different depths in the atmosphere. We obtained the number of secondary particles, its fluctuations, and the energy distribution of secondaries, for gamma-initiated sub-showers in the energy range 10–10^5 GeV, and for electrons-initiated sub-showers in the energy range 10–10^4 GeV, as a function of atmospheric depth ranging up to about 27 X_0. The motivation to limit the energy range of electron-initiated sub-showers with respect to the case of gamma-initiated ones stems from an analysis of the energy distribution of secondary particles in EAS according to the HEMAS

* Corresponding author. E-mail: patera@hpserver.lnf.infn.it.

SSDI 0168-9002(94)01315-2

simulation code [5]. The above mentioned features of the electromagnetic cascade allow to express the results in terms of the total thickness expressed in radiation length, independently from X_{detector} and X_{start}.

We remark the importance of taking into account fluctuations. As already reported by other authors [6], biases are introduced in the final results when using only the average values. This is due to the non-symmetric shape of distributions of the number of secondary particles.

In the next section we describe the simulation tools. The results are then reported in Section 3.

2. The simulation

Among the shower programs available in the high energy physics community, we have adopted GEANT version 3.15 [7] and FLUKA [8]. For primary energy greater than a few TeV FLUKA has been mainly used, since there GEANT starts to exit from its range of validity. We have verified that at the boundary energies around 10^3 GeV the results of the two generators in air are reasonably compatible, as discussed later.

The simulations have been performed on different platforms (HP-UX, IBM-AIX, VAX, and ALPHA DECStations).

The atmosphere is defined by a stack of box volumes of rectangular basis and thickness increasing with the

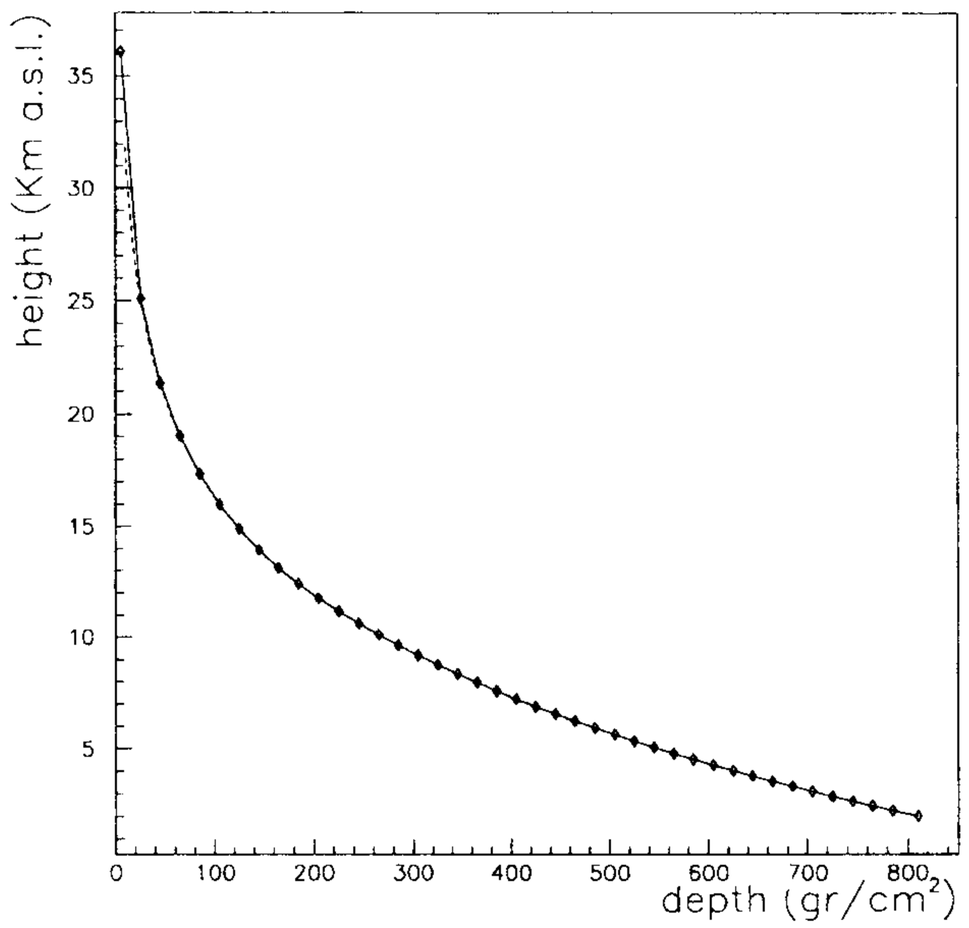

Fig. 1. The profile of the standard atmosphere used in the simulation set-up. The solid line is the adopted piece-wise linear approximation.

height above the sea level. Any volume corresponds to a depth scaled for the density equal to $\simeq 24$ g/cm^2. In each box the density is uniform, and it is chosen in such a way that an approximation to the standard US atmosphere is performed according to the Shibata fit [9]. The chosen

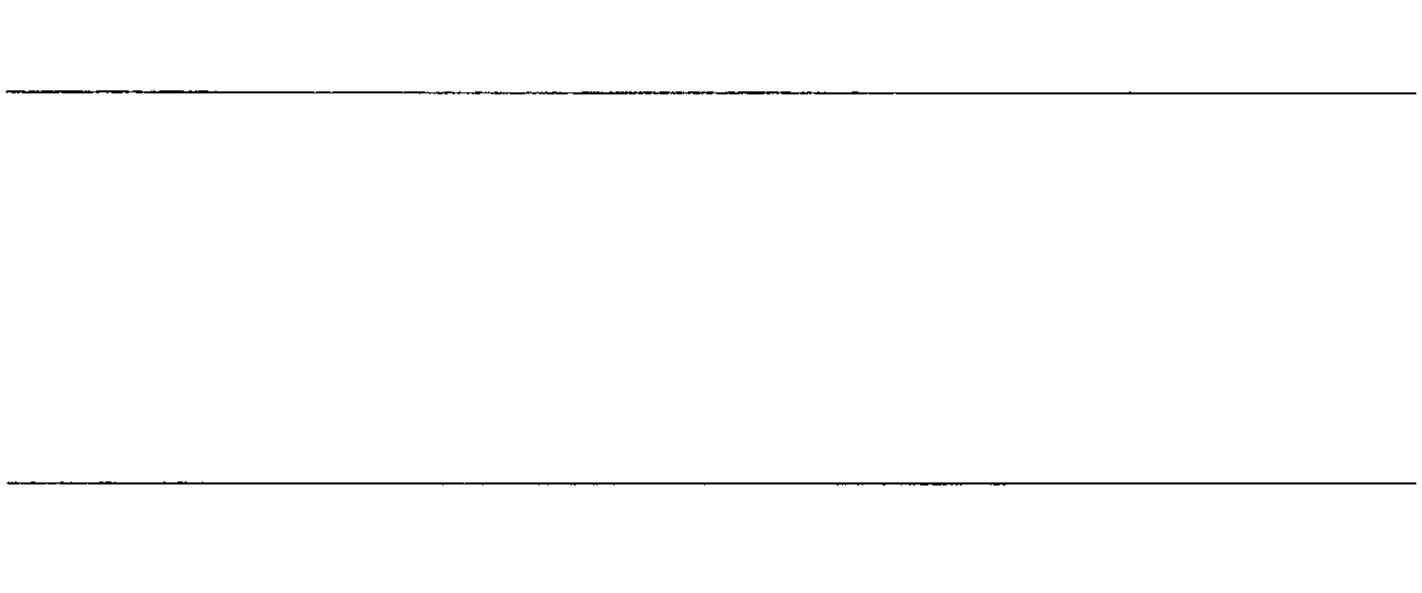

Fig. 2. A 300 GeV electron shower in atmosphere, initiated at 60 g/cm^2, as simulated using GEANT (only secondaries with energy greater than 500 MeV are shown). The box structure reproducing the atmosphere, from 2 km to 36 km above sea level, is shown: each layer has a thickness of about 0.5 X_0. The horizontal scale is enlarged by a factor of 100 with respect to the vertical.

depth granularity in our approximation is about one about one half of radiation length (37.66 g/cm^2) in air. The exact relation between height and slant depth in Fig. 1, with the polygonal representing our approximation.

We have limited the top of atmosphere at 5 g/cm^2 (corresponding to a vertical height of $\simeq 36$ km), and the bottom is at 1025 g/cm^2 (corresponding to the sea level). We have used the same elemental composition at all depths.

We have fixed the kinetic energy cut for secondary particles to 1 MeV. This is an improvement with respect to the results of Ref. [10], where the lowest considered cut, for electrons, was 5 MeV. It turns our that, in practice, a 1 MeV threshold is a reasonable compromise, taking into account both the quality of the results and the required computer time. In fact, one has to consider that real detectors are often shielded by an amount of material capable of absorbing most of the low energy (less than 1 MeV) secondary electrons. The matter could be different, in principle, for low energy secondary photons which have a longer transmission coefficient, but the electrons are those which are responsible for most of the energy deposition in an active material.

At very high energy we made use of the possibility offered by FLUKA to exploit biasing techniques in order to explore with good accuracy the longitudinal profile in a reasonable time, although this did not allow to measure the correct fluctuations, which were studied with analogical simulations at lower statistics.

We also did not change the energy threshold in the different air layers, otherwise it would not have be possible to parametrize the results as a function of the atmospheric thickness expressed in radiation lengths, independently from X_{detector} and X_{start}, taken separately.

An example of the simulation set-up is given in Fig. 2 which shows the development of a shower initiated by an electron of 300 GeV starting at a vertical atmospheric depth of 60 g/cm^2; only secondary tracks with energy greater than 500 MeV are shown for clarity. In order to achieve a reliable parametrization of the relevant shower properties, we generated sub-shower at different log-spaced energies: 10, 18, 31, 56, 100, 177, 316, 562, 1000, 1778, 3128, 5623, 10 000, 17 780, 31 620, 56 230, 100 000 GeV (the last four values have been omitted for electron showers), and at 16 different starting depths: from 10 to 910 g/cm^2, in 60 g/cm^2 steps.

3. Results

We have considered as interesting quantities the longitudinal profile together with the associated fluctuations, the energy distribution of secondary particles above the Monte Carlo cut, and their lateral distribution. In this paper we shall not explore the details of the lateral distribution, limiting ourselves to some general considerations. This topic will be treated separately in a forthcoming dedicated paper together with the analysis of arrival times and of their fluctuations as a function of radial distance from the shower axis.

We have fitted the Monte Carlo results with phenomenological parametrizations, trying to minimize as much as possible the number of parameters. Whenever possible we started from the analytical expressions already existing in the literature, so that the possible differences with respect to the simplified shower theory could emerge naturally.

3.1. Longitudinal profiles

We sample the longitudinal profile by counting the number of secondary particles crossing the boundary between the adjacent air regions in our simulation set-up. We have fitted the number of secondary e^+e^- or photons, with energy greater or equal to the Monte Carlo cut (1 MeV) using a six parameters expression similar to that proposed by Greisen [14]:

$$\langle N_{e,\gamma}(E_0, t)\rangle = C_1 \beta^{C_2} e^{t_1(C_5 - C_6 \log s_1)}, \tag{1}$$

where

$$t_1 = t + C_4, \tag{2}$$

$$\beta = \log\left(\frac{E_{\text{primary}}}{\epsilon_C}\right), \tag{3}$$

$$s_1 = \frac{3t_1}{t_1 + C_3\beta}, \tag{4}$$

t being the atmospheric depth expressed in radiation lengths, and ϵ_C the critical energy in atmosphere: ~ 81 MeV. The variable s_1 is therefore a slightly modified "age" parameter. The exact definition of the age parameter can be found in the quoted Ref. [14], we just remind here that it is an dimensionless number emerging in the analytical treatment of atmospheric showers. It ranges

Table 1
Parameters of the fit to the longitudinal shower profiles for gamma-initiated sub-showers

Secondary	C_1	C_2	C_3	C_4	C_5	C_6
e^+e^-	0.21915	−0.38502	1.7709	−0.041189	1.1189	1.5532
γ	0.85721	−0.15412	1.9988	−0.43781	0.97262	1.4218

Table 2
Parameters of the fit to the longitudinal shower profiles for electron-initiated sub-showers

Secondary	C_1	C_2	C_3	C_4	C_5	C_6
e^+e^-	0.33499	−0.73003	1.4908	0.3046	1.3639	1.7703
γ	1.169	−0.34014	1.7893	−0.076683	1.0986	1.5324

approximately between 0.5 and 2.0, according to the distance from the first interaction, reaching the unit value at the shower maximum.

We want to remark that this single formula is able to provide a good approximation of the longitudinal profiles in the whole considered energy range (5 order of magnitude).

All C_i $(I = 1, 2, \cdots, 6)$ parameters depend upon both primary and secondary nature. They are given in Tables 1 and 2.

An example of the quality of the fits to the longitudinal profiles for a few primary energies is given in Figs. 3 and 4 for photon- and electron-initiated sub-showers respectively. Some systematic tendency to underestimate the real profile may appear beyond the shower maximum, in particular for γ secondaries at the lower primary energies. However, we have verified that such deviations are within the fluctuations of the performed simulation.

It is interesting to notice how C_5 is always not far from 1, and C_6 is about $\frac{3}{2}$, as expected in Greisen theory. Instead the meaning of parameter C_4 is linked to the known differences in shower development for electrons and photons.

From expression (1) we also derive the position of shower maximum as a function of energy:

$$t_{\max} = \frac{(1 + x_m)C_3\,\beta}{2 - x_m} - C_4, \tag{5}$$

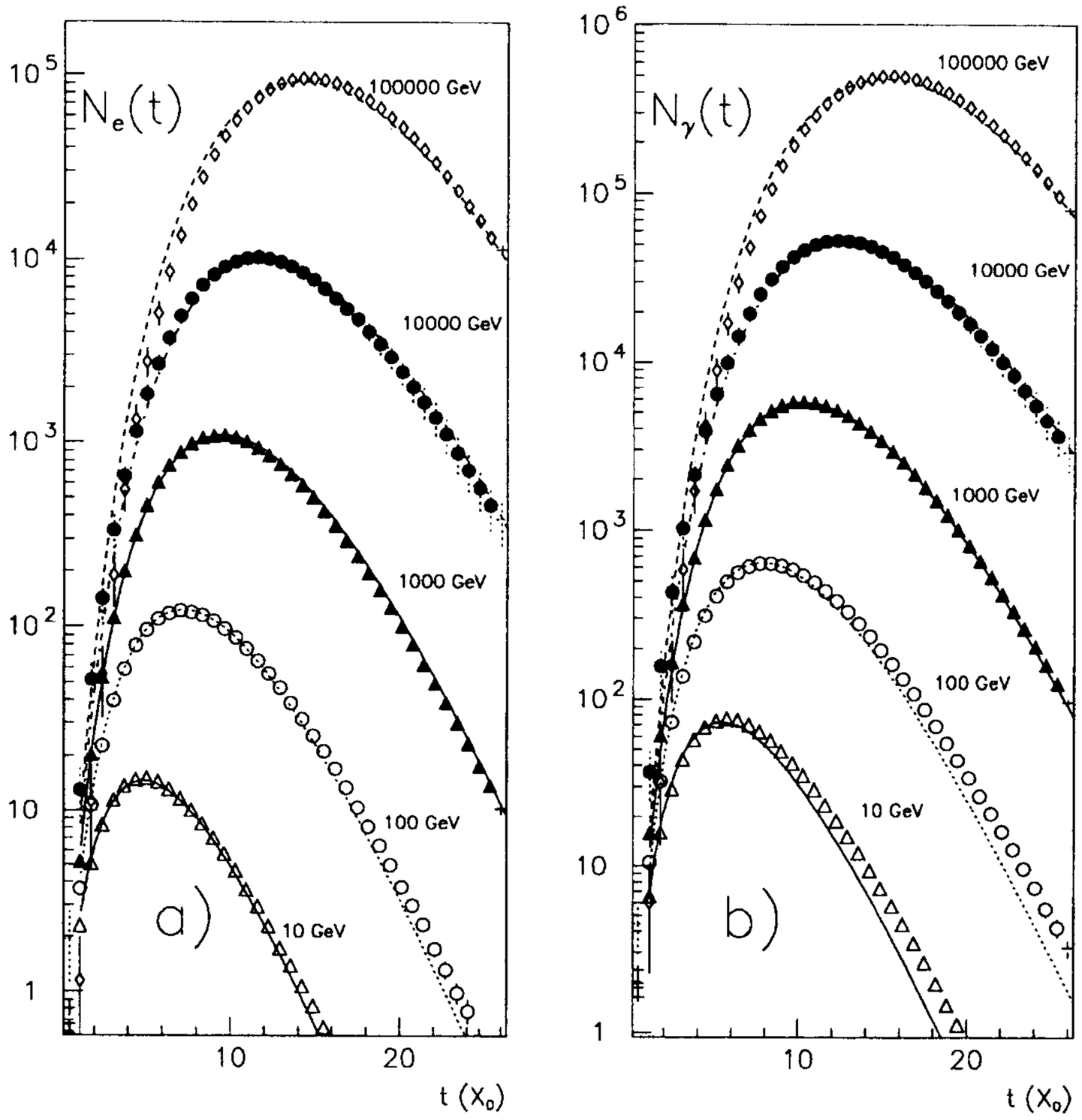

Fig. 3. (a) Longitudinal profiles of secondary electron/positrons from gamma-initiated sub-showers, 0.01, 0.1, 1, 10, and 100 TeV primary energy; (b) longitudinal profiles of secondary photons. The results of expression (1) are superimposed.

where

$$x_m = \frac{2}{3}\left(1 - \sqrt{4 - \frac{9}{2}\frac{C_5}{C_6}}\right). \quad (6)$$

The above formulae are obtained knowing that around the maximum $s_1 = 1 + x_m$, with $x_m \ll 1$, and then using the Taylor expansion of $\log(1+x)$ up to second order. As expected t_{max} grows linearly with β, i.e. with $\log E_0$.

In Fig. 5 we show the depth at which the shower maximum is reached in the Monte Carlo results, as a function of $\log_{10} E_0$, for gamma-initiated sub-showers. In the region 1–10 TeV the results of GEANT and FLUKA are superimposed. It can be noticed how the GEANT results start to deviate from the expected linear behaviour after a few TeV. At lower energy both codes give, with remarkable approximation, the same results, as shown in Fig. 6 for 1 TeV gamma-initiated sub-showers.

We conclude this section remarking the importance of the secondary photons. From Fig. 4 and Fig. 3 can be easily seen that the gamma component of an EAS overwhelms by almost an order of magnitude the number of electrons. The fraction of energy deposition in the sensitive material due to these photons will depend of course on the atomic characteristics of the medium and on its thickness.

3.2. Fluctuations

In order to parametrize the fluctuations on the number of secondary particles, we have tried, at phenomenological level, to take into account the fluctuations on the starting point of the showers. This brings naturally to search for a function of the age parameter as suggested in Ref. [3]. However, a Poisson-like term seems unavoidable, in particular beyond the shower maximum. Valuable results have been obtained by us using the following expression:

$$\frac{\sigma^2_{Ne,\gamma(E_0,t)}}{\langle N_{e,\gamma}(E_0, t)\rangle^2} = k_1^2\left[s_1 - k_1 - k_3 \log(s_1)\right]^2 + \frac{k_4}{\langle N_{e,\gamma}(E_0, t)\rangle}, \quad (7)$$

where $\langle N_{e,\gamma}(t)\rangle$ and s_1 are respectively the average number of secondaries and the modified age parameter as defined in Section 3.1. The k_i factors are functions of

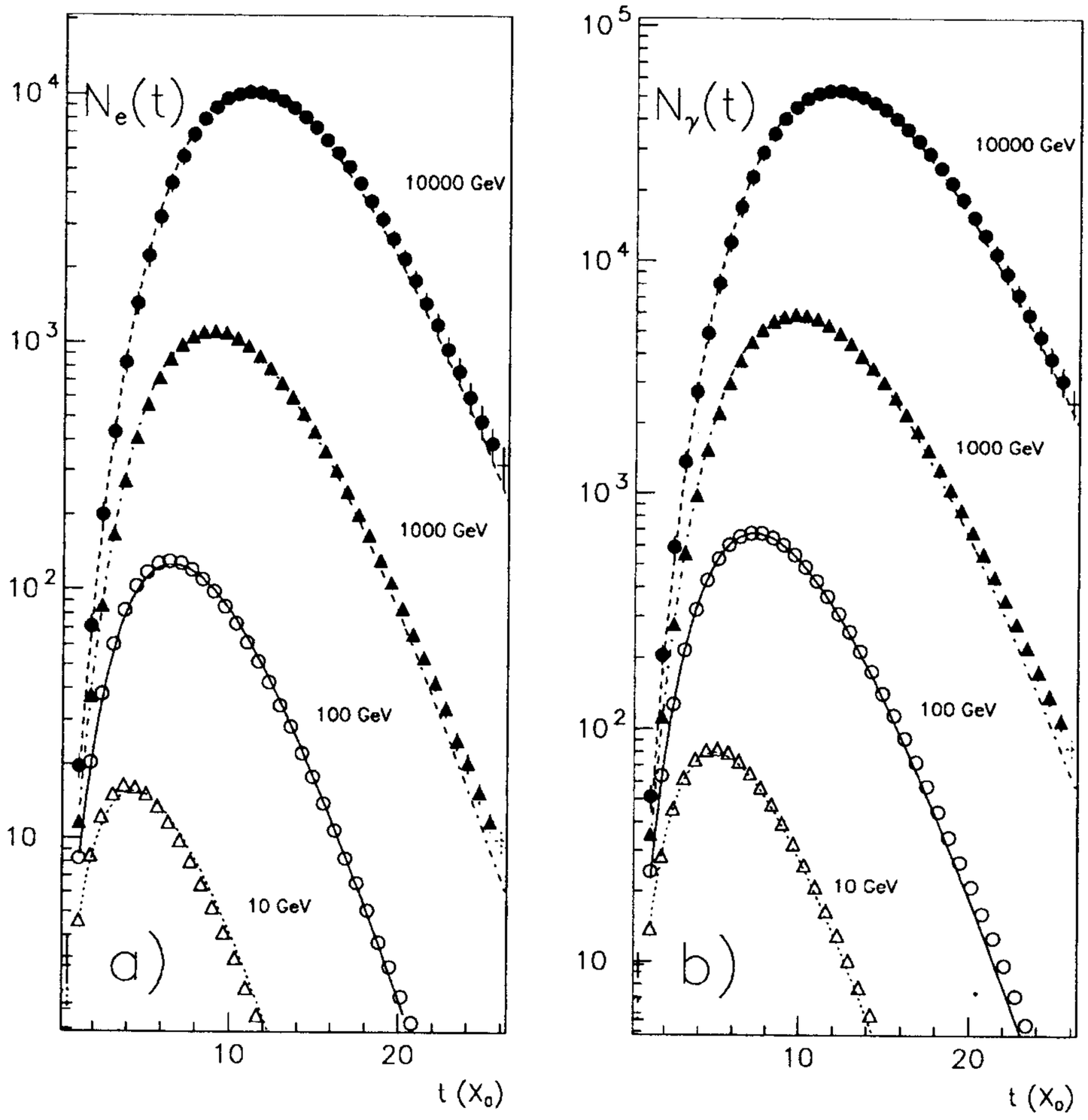

Fig. 4. (a) Longitudinal profiles of secondary electron/positrons from electron-initiated sub-showers, 0.01, 0.1, 1, and 10 TeV primary energy; (b) longitudinal profiles of secondary photons. The results of expression (1) are superimposed.

primary energy, and depend also on the nature of primary and secondary particles. Examples of the results are summarized in Figs. 7 and 8 for gamma- and electron-initiated sub-showers respectively.

In order to make use of these parametrizations, one has to consider that the number of secondary particles is log-normally distributed, with good approximation. It can be easily shown that the following relations hold [15]:

$$\sigma^2_{\log N} = \log\left[\frac{\sigma_N^2}{\langle N\rangle^2} + 1\right], \tag{8}$$

$$\langle \log\ N\rangle = \log\langle N\rangle - \frac{\sigma^2_{\log N}}{2}. \tag{9}$$

The k_i parameters with $i = 1, 2, 3$ can be defined as polynomials of the variable $y = \log_{10}(E_0)$:

$$k_i = W_0^i + W_1^7 y + W_2^i y^2 \quad i = 1, 2, 3, \tag{10}$$

while for the 4th parameter k_4 we have:

$$k_4 = \exp\left(W_0^4 + W_1^4 y + W_2^4 y^2\right). \tag{11}$$

The W_i^j parameters are given in Tables 3 and 4 for γ and e^+e^- primaries and secondaries.

3.3. Energy distributions

The energy distribution of secondaries at a given depth depends on the radial distance from the shower axis. As a first approximation we integrate over the total area. We assume that the knowledge of the average energy is sufficient to determine the energy deposition in a given detector (for instance a scintillator). We remind in fact that for the aim of this work, the transverse dimensions of an e.m. sub-shower are in general much smaller than those of the whole EAS.

We have found that the energy distributions of secondary particles, at a given depth, are well approximated by the following expression:

$$\frac{\mathrm{d}N_{e,\gamma}(E_0, t)}{\mathrm{d}E} = CE^{\alpha(t)}\, \mathrm{e}^{\beta(E_0,t)E^{\gamma(t)}}, \tag{12}$$

where C is simply a normalisation constant, E_0 is the primary energy, and t is the atmospheric depth. Such an expression starts to underestimate the real distribution when this has decreased by at least two order of magnitude from the peak value.

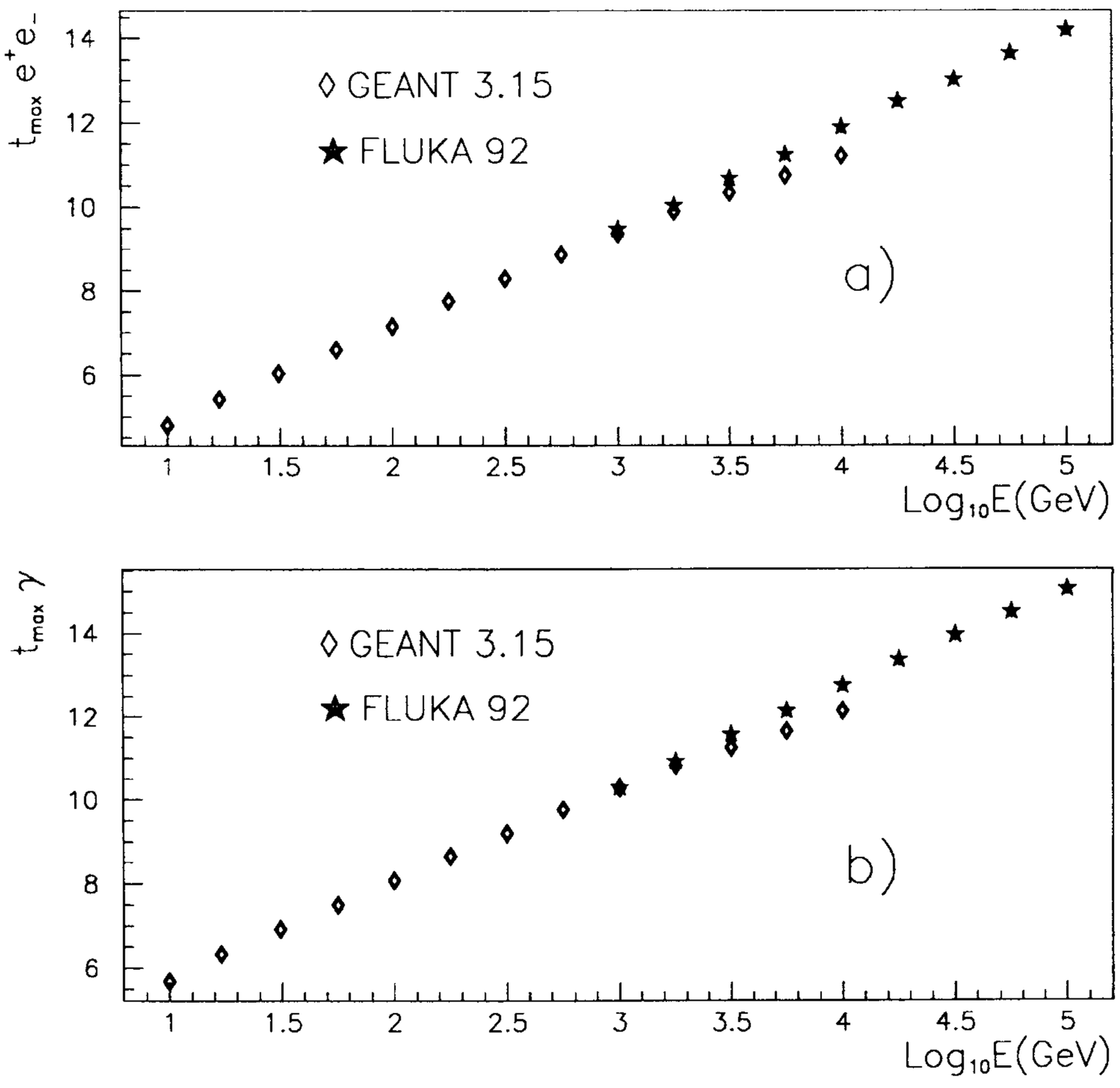

Fig. 5. Atmospheric depth at which the shower maximum is reached, as a function of $\log_{10} E_0$, for gamma-initiated sub-showers; (a) secondary e^+e^-, (b) secondary γ. In the energy region 10^3–10^4 GeV GEANT and FLUKA results are superimposed: FLUKA is able to maintain the linear behaviour even at these high energies.

Table 3
Fit parameters for the fluctuations of the longitudinal profile for γ-initiated sub-showers

Coeff.	e^+e^- secondary			photons secondary		
	W_0	W_1	W_2	W_0	W_1	W_2
k_1	1.81	0	0	1.31	3.38×10^{-1}	-6.22×10^{-2}
k_2	1.19	-3.00×10^{-2}	0	1.21	-6.38×10^{-1}	4.92×10^{-3}
k_3	2.94×10^{-1}	4.30×10^{-2}	0	2.80×10^{-1}	3.30×10^{-2}	0
k_4	-2.99×10^{-1}	1.07	0	1.81×10^{-1}	1.39	0

The expressions α, β, and γ are functions of t and E_0, and depend upon the nature of both primary and secondary particles. Examples of the obtained results are given in Figs. 9 and 10 for 562 GeV sub-showers initiated by gamma and electrons respectively.

We also notice how the knowledge of the energy distribution allows to scale the above mentioned longitudinal profiles down to any value of energy cut greater than 1 MeV.

In the following we give the parametrization of all relevant functions for the four different cases. The variables $y = \log_{10} E_0$ and $x = 810 - 30.570t$ are introduced.

3.3.1. Secondary e^+e^- from primary photons

$$\alpha(x) = -0.4602 + 0.1458 \times 10^{-4}\, x, \tag{13}$$

$$\beta(E_0, x) = p_0(E_0) + p_1(E_0)x, \tag{14}$$

where p_0 and p_1 are given by:

$$p_0 = 34.692 - 2.47085y - 1.6181\,y^2 + 0.32336\,y^3, \tag{15}$$

$$p_1 = -0.32205 \times 10^{-1} - 1.8219 \times 10^{-3}y + 4.06915 \times 10^{-3}y^2 - 6.7065 \times 10^{-4}y^3. \tag{16}$$

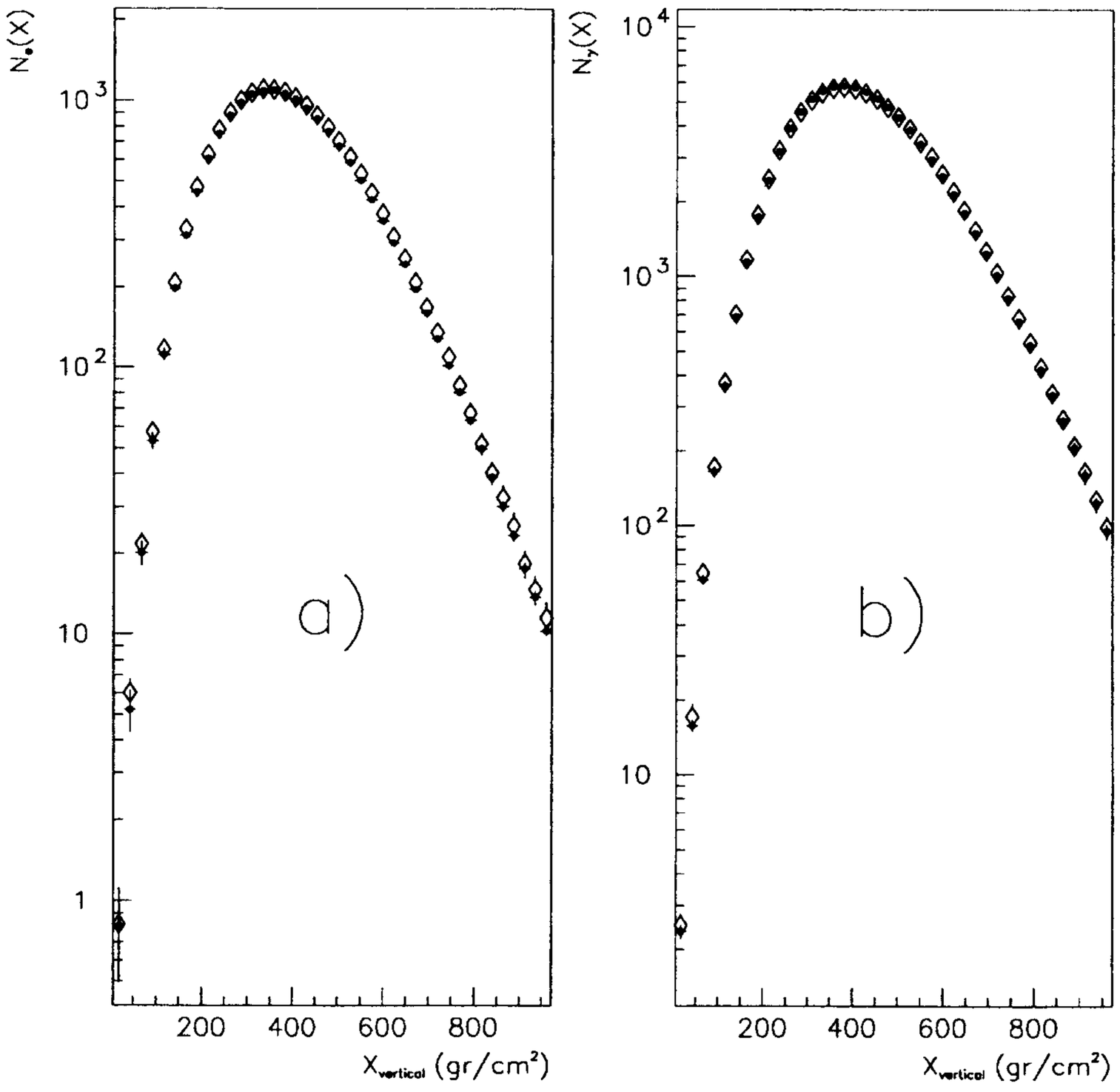

Fig. 6. Longitudinal profiles of secondary electrons (a), and of secondary photons (b), for simulated 1 TeV gamma-initiated sub-showers, as a function of atmospheric depth. Black symbols are the GEANT results, while the open ones are from FLUKA.

Table 4
Fit parameters for the fluctuations of the longitudinal profile for e^+e^--initiated sub-showers

Coeff.	e^+e^- secondary			photons secondary		
	W_0	W_1	$W_2 \times 10^3$	W_0	W_1	$W_2 \times 10^3$
k_1	2.97	-5.58×10^{-1}	49.4	1.72	1.13×10^{-1}	−46.2
k_2	1.04	4.25×10^{-2}	−6.77	1.13	-2.20×10^{-2}	2.28
k_3	9.30×10^{-1}	-1.11×10^{-1}	9.75	6.67×10^{-1}	2.49×10^{-3}	−8.19
k_4	1.96×10^{-1}	2.73×10^{-1}	161	-1.74×10^{-1}	1.34	−1.34

In this case γ is a constant:

$$\gamma = 0.87. \tag{17}$$

3.3.2. Secondary γ from primary photons

$$\alpha(x) = -0.81356 - 0.11373 \times 10^{-3}x, \tag{18}$$

$$\beta(E_0, x) = c(E_0)(0.229845 - 3.5588 \times 10^{-2}x + 1.6177 \times 10^{-5}x^2 - 6.608 \times 10^{-9}x^3), \tag{19}$$

where

$$c(E_0) = 1.1308 - 0.058528\,y, \tag{20}$$

$$\gamma(x) = 0.8856100 - 0.44941 \times 10^{-3}x + 0.30669 \times 10^{-6}x^2 - 0.13216 \times 10^{-9}x^3. \tag{21}$$

3.3.3. Secondary e^+e^- from primary electrons

$$\alpha(x) = -0.488 + 0.56271 \times 10^{-4}x, \tag{22}$$

$$\beta(E_0, x) = p_0(E_0) + p_1(E_0)x, \tag{23}$$

where p_0 and p_1 are given by:

$$p_0 = 58.475 - 2.5329\,y + 6.0455\,y^2 - 5.3685 \times 10^{-1}y^3, \tag{24}$$

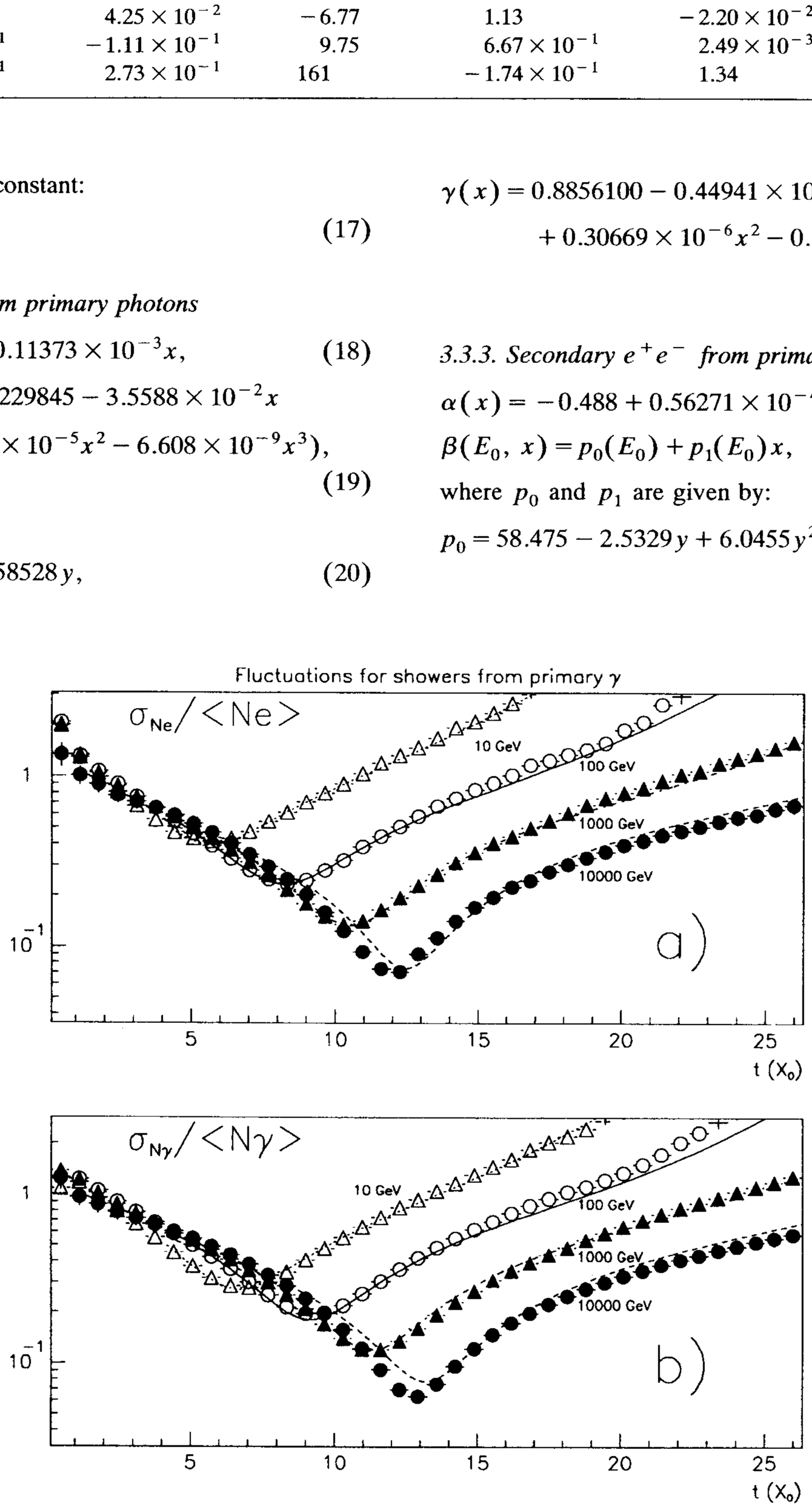

Fig. 7. Relative fluctuations of of secondary e^+e^- (a) and γ (b) ($E \geq 1$ MeV) for gamma initiated sub-showers as a function of atmospheric depth in r.l.

$$p_1 = -6.634 \times 10^{-2} + 3.2933 \times 10^{-2} y - 2.513 \times 10^{-2} y^2 + 6.741 \times 10^{-4} y^3. \quad (25)$$

Also in this case γ is a constant:

$$\gamma = 0.89. \quad (26)$$

3.3.4. Secondary γ from primary electrons

$$\alpha(x) = -0.8846 - 0.7472 \times 10^{-4} x, \quad (27)$$

$$\beta(E_0, x) = p_0 + p_1 x + p_2 x^2 + p_3 x^3, \quad (28)$$

where p_0, p_1, p_2, and p_3 are given by

$$p_0 = 50.235 - 13.144 y + 1.70655 y^2 + 3.49745 \times 10^{-4} y^3, \quad (29)$$

$$p_1 = -1.54705 \times 10^{-1} + 5.475 \times 10^{-2} y + 1.3477 \times 10^{-3} y^2 - 1.7199 \times 10^{-3} y^3, \quad (30)$$

$$p_2 = 3.12305 \times 10^{-4} - 7.5745 \times 10^{-5} y - 2.43885 \times 10^{-5} y^2 + 6.6675 \times 10^{-6} y^3, \quad (31)$$

$$p_3 = -2.3047 \times 10^{-7} + 3.1436 \times 10^{-8} y + 2.6297 \times 10^{-8} y^2 - 5.812 \times 10^{-9} y^3, \quad (32)$$

while γ is now:

$$\gamma = 1.0. \quad (33)$$

3.4. Comparison with previous results in literature

The e.m. component of EAS has been extensively studied during the last 40 years. However, in spite of the huge number of published papers on the features of the secondary electrons, very few results exist (to our knowledge) on the generated gammas. In this section we compare our result to some of the many papers available on the electron component of E.A.S. and to the few results on secondary gammas.

The most straightforward comparison is the average number of secondary produced in EAS. We typically found a good agreement with results in literature.

As example in Fig. 11 we compare the obtained average number of secondary electrons with energy greater than 5 MeV produced by a 1 TeV γ primary to the parametrizations found in refs. [10,11].

As stated before, the lack of published results makes the comparison more problematic for the secondary gammas shower profile. There is the very old work from

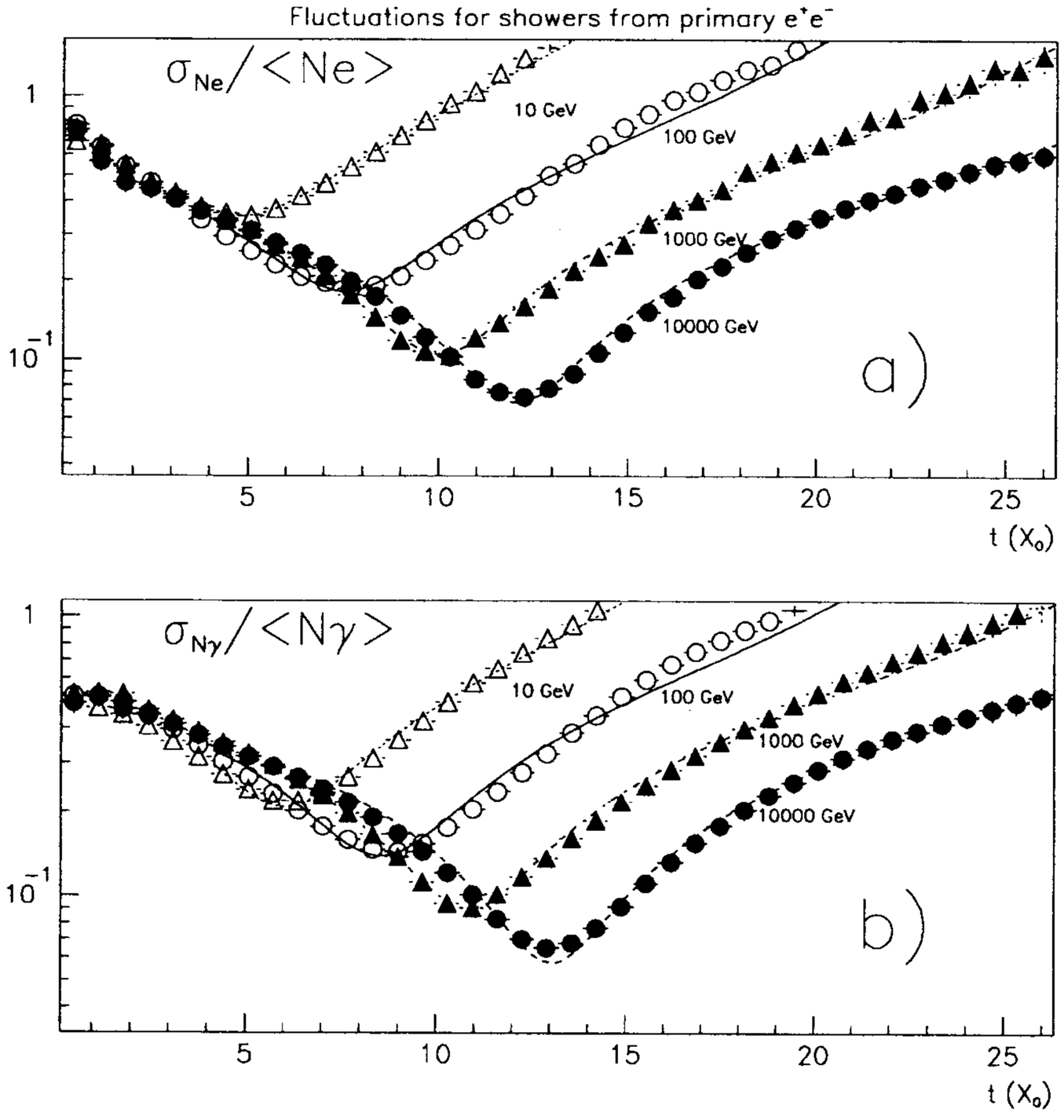

Fig. 8. Relative fluctuations of of secondary e^+e^- (a) and γ (b) ($E \geq 1$ MeV) for electron initiated sub-showers as a function of atmospheric depth in r.l.

Messel and Crawford [12] and some results in the more recent papers in [6,13].

We found a macroscopic discrepancy between Messel and Crawford and the numbers obtained by all the other authors (ours included) both for the numbers of gammas and for the depth at which the maximum number of gamma is obtained in the shower. In particular, it is hard to understand the large difference in radiation lengths between the position of shower maximum for secondary electrons and that of secondary gammas as given in Ref. [12]. On the other hand, our results seem to agree very well with the profile of secondary gammas produced by

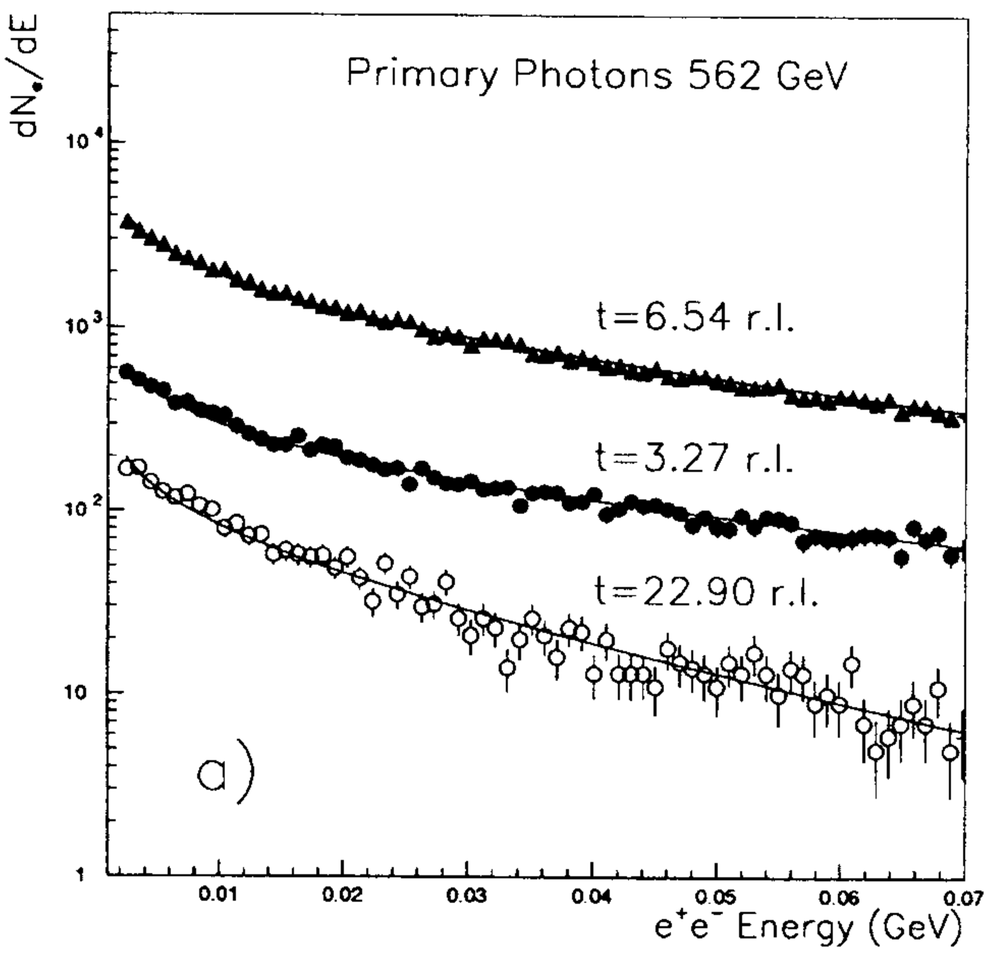

Fig. 9. Energy distribution of secondary electrons (a), and photons (b), for photon-initiated sub-showers at 562 GeV at three different atmospheric depths.

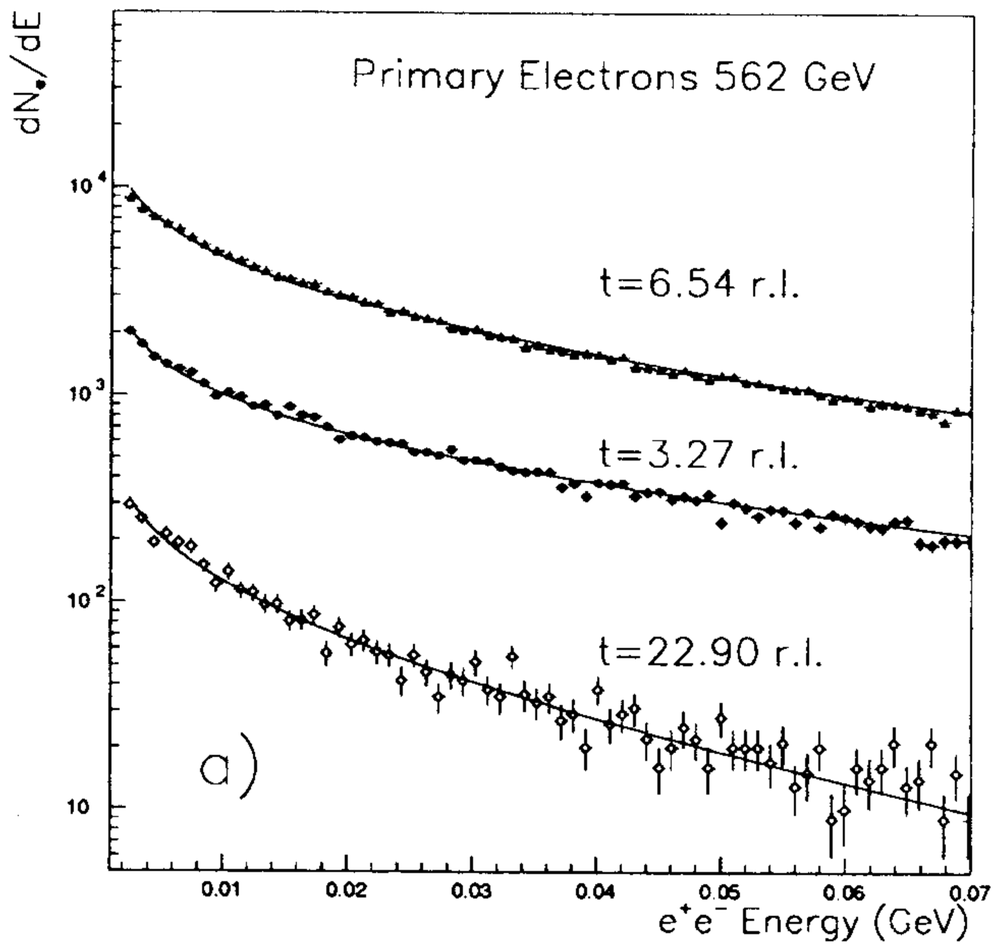

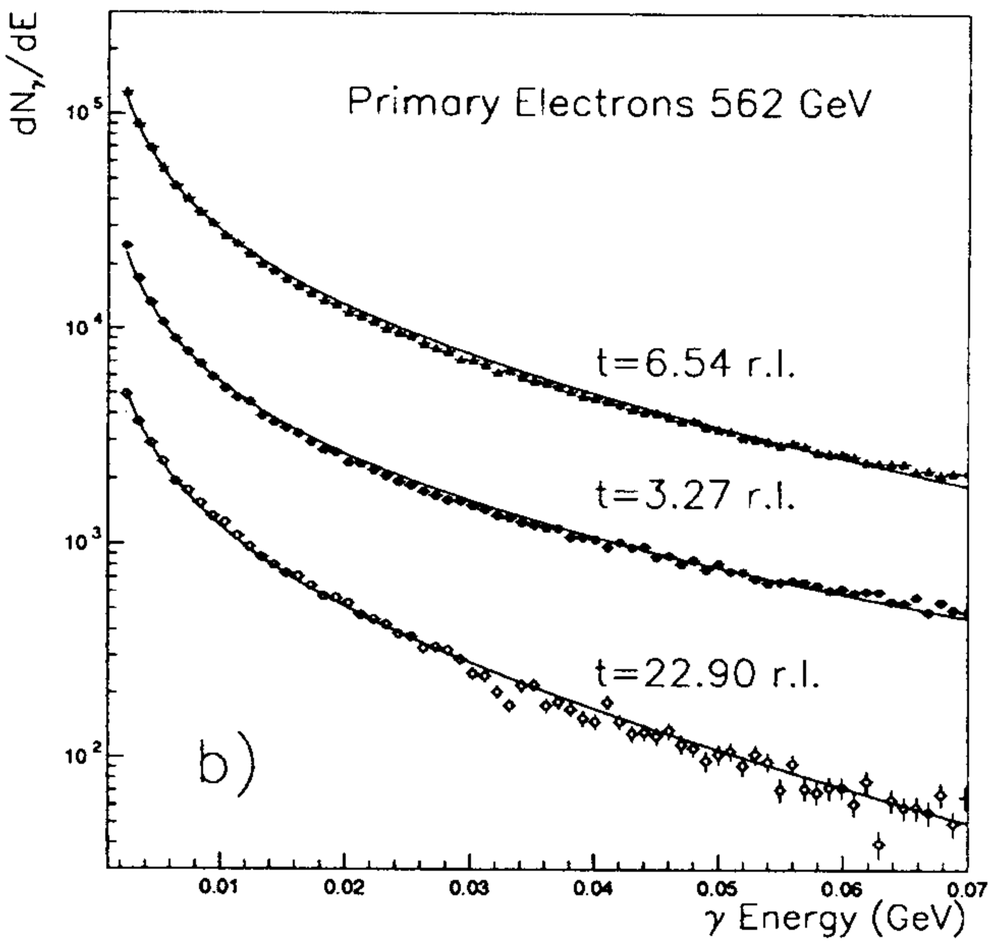

Fig. 10. Energy distribution of secondary electrons (a), and photons (b), for electron-initiated sub-showers at 562 GeV at three different atmospheric depths.

100 GeV and 1 TeV electron primary computed in Ref. [6], and qualitatively well with the only point in Ref. [13] within the range of primary energy and depth explored also by us.

In Fig. 12 we show the fluctuations of the secondary electrons with 5 MeV minimum energy produced by 100 GeV and 1 TeV gamma primary, superimposed to the results of Ref. [11]. The agreement seems good, expecially in the region of maximum development of the shower. In Table 5 we report the secondary electrons fluctuations for a threshold energy of 1.5 MeV and for 100 GeV and 1

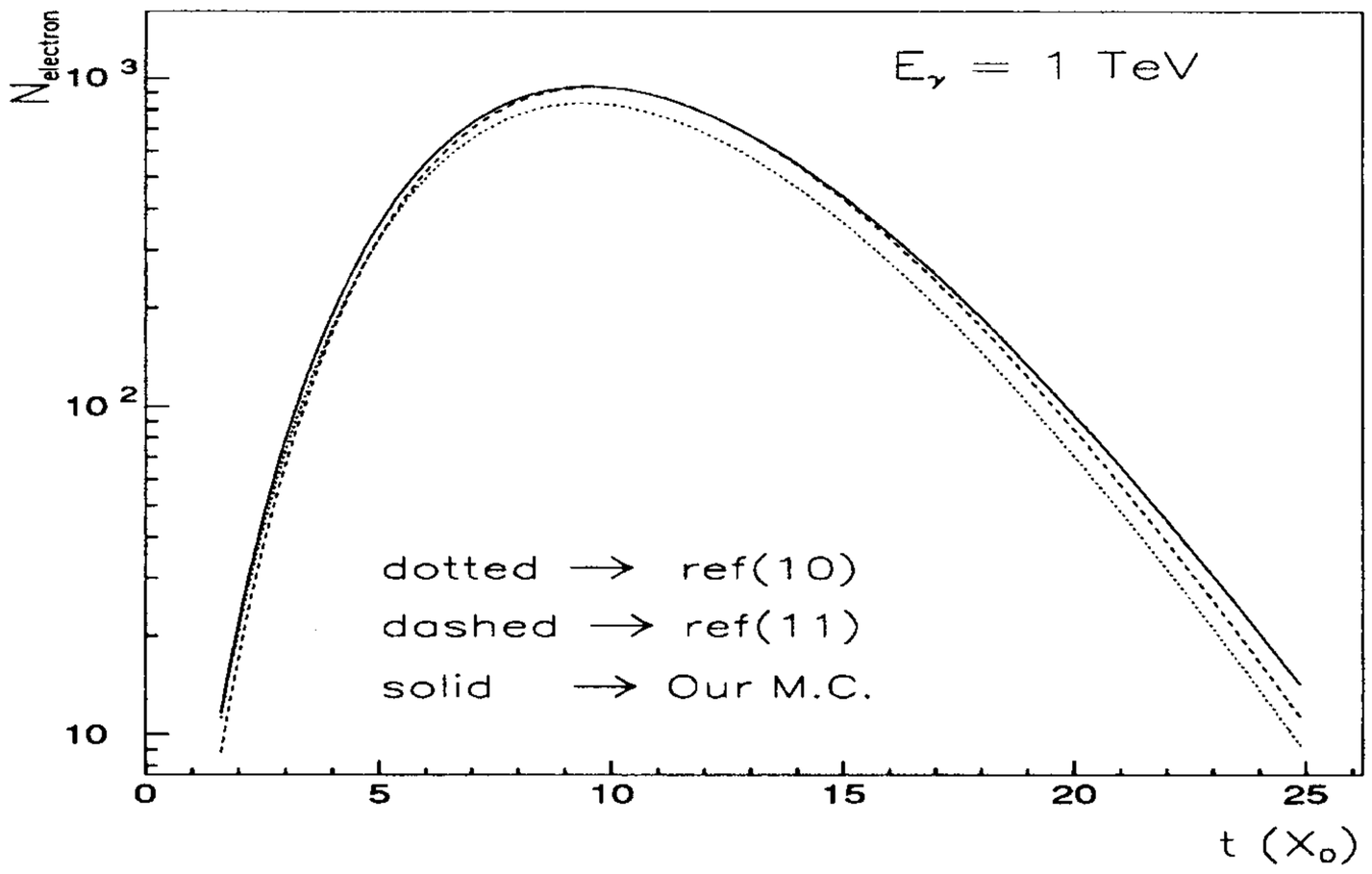

Fig. 11. Comparison of the average number of secondary electrons with energy greater then 5 MeV generated by a 1 TeV gamma primary according to Refs. [10,11] and to our MC.

TeV primary electrons. It can be seen that our fluctuations are slightly bigger than those reported in Ref. [6].

3.5. Lateral distribution

As expected the lateral distribution of secondary particles on a plane perpendicular to the shower axis is fitted, with reasonable approximation, by the Nishimura–Kamata–Greisen function [14]:

$$f(x) = N_e \frac{\Gamma(4.5-s)}{2\pi\Gamma(s)\Gamma(4.5-2s)} x^{s-2}(1+x)^{s-4.5}, \tag{34}$$

where $x = r/r_0$. The parameters r_0 and s, are derived from the fit, are really close to the expected Moliere radius and age parameter respectively. An example of fit is shown in Fig. 13, for secondary e^+e^- in a 1 TeV gamma initiated sub-shower, after an atmospheric depth of 460 gr/cm^2. This kind of function starts to overestimate the real distribution only at very large distances from the shower axis.

4. Conclusions

A successful parametrization of some relevant features of e.m. showers in atmosphere has been presented. The

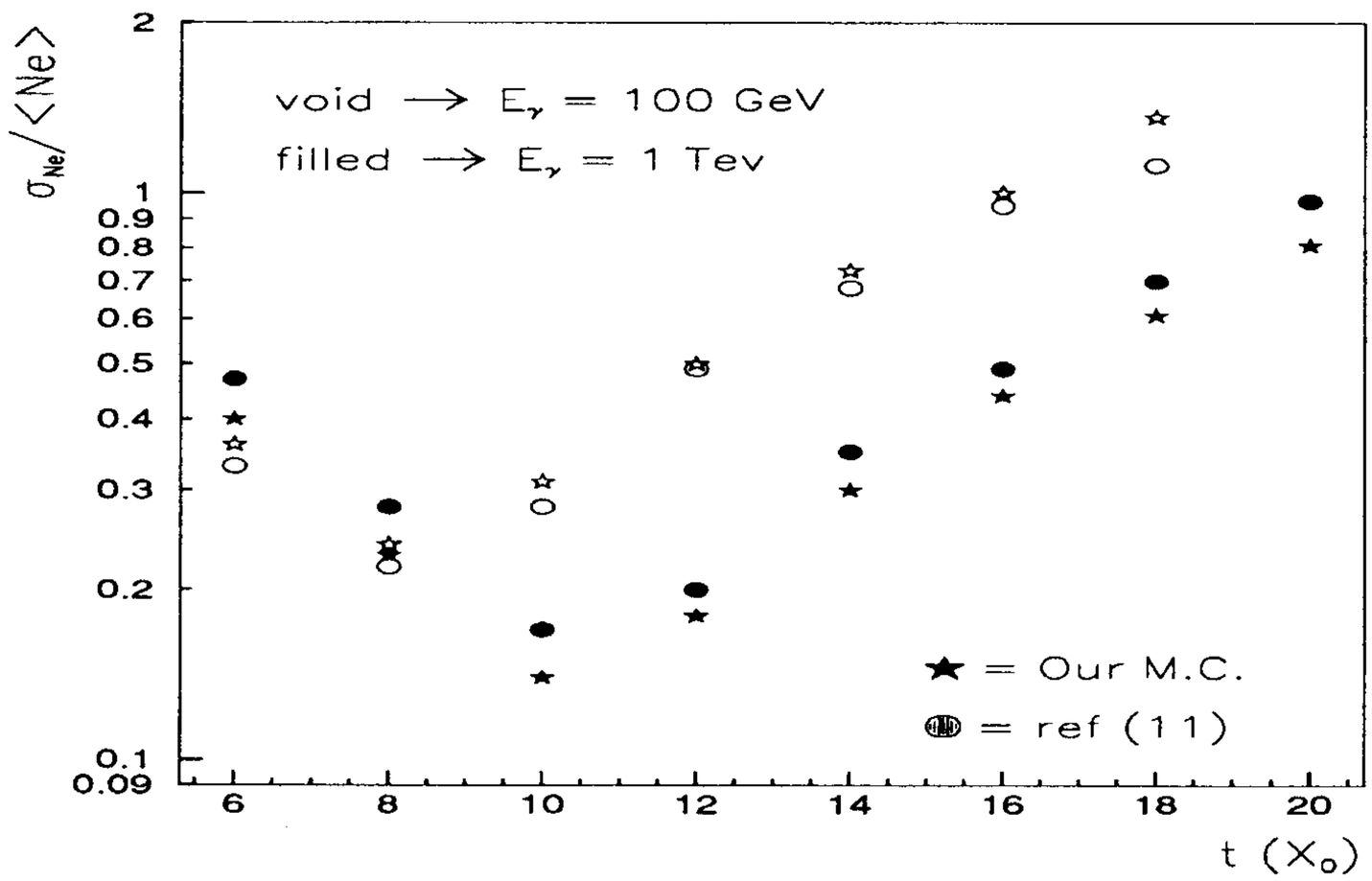

Fig. 12. Fluctuation of the number of secondary electrons with threshold energy of 5 MeV generated by 100 GeV and 1 TeV gamma according to Ref. [11] and to our MC.

Table 5
Comparison of the fluctuation of number of electrons ($\sigma N/N$) with threshold energy 1.5 MeV to the results in Ref. [6]

E_{prim}		2 r.l.	4 r.l.	6 r.l.	8 r.l.	10 r.l.
100 GeV	Our MC.	0.5	0.32	0.21	0.19	0.26
100 GeV	Ref. [6]	0.46	0.26	0.15	0.17	0.3
1000 GeV	Our MC.	0.51	0.36	0.26	0.16	0.10
1000 GeV	Ref. [6]	0.45	0.33	0.2	0.12	0.11

aim of this work is to provide a set of tools to achieve fast and reliable simulation of the e.m. component of EAS for the analysis of cosmic ray physics. In future papers we plan to extend such a work to a detailed analysis of lateral distribution and of the arrival time fluctuations.

A dedicated effort will be reserved for the parametrization of the e.m. component of hadronic sub-showers.

All correspondence can be sent to the following e-mail addresses:
patera@hpserver.lnf.infn.it
battist@hpserver.lnf.infn.it
carboni@hpserver.lnf.infn.it
ferraria@cernvm.cern.ch

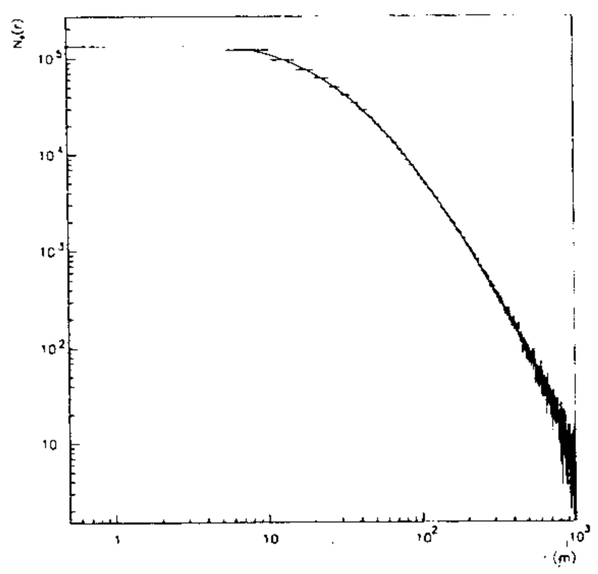

Fig. 13. Radial distribution of secondary $e^+ e^-$ ($E \geq 1$ MeV) for a 1 TeV gamma shower after 460 gr/cm^2. The fit to a NKG function is shown.

Acknowledgements

Part of this work has been carried on by one of us (V.P.) at the California Institute of Technology. He wishes to express his gratitude to Prof. B. Barish and his coworkers for their kind hospitality. We are indebted to Prof. G. Navarra, Dr. S. Coutu and Dr. P. Vallania for many useful discussions.

References

[1] D. Müller et al., Proc. 22nd ICRC, Dublin (Ireland) 1991, OG 6.1.12, Vols. 2, 25 and references therein.
[2] See for instance G. Battistoni, Simulations in High Energy Cosmic Ray Physics, Proc. 4th Int. Conf. on Calorimetry in High Energy Physics, La Biodola (Is. d'Elba), Italy, Sept. 20–25 1993, eds. A. Menzione and A. Scribano (World Scientific) p. 493.
[3] T.K. Gaisser, Cosmic Rays and Particle Physics, (Cambridge University Press, Cambridge 1990) chap. 15 and references therein.
[4] B. Rossi and K. Greisen, Rev. Mod. Phys. 13 (1941) 240.
[5] C. Forti et al., Phys. Rev. D 42 (1990) 3668.
[6] H.P. Vankov and T. Stanev, Astron. Phys. 2 (1994) 35.
[7] R. Brun et al., CERN GEANT 3 User's Guide, DD/EE/84-1 (1987).
[8] A. Fassó et al., Fluka: Present Status and Future Developments, Proc. 4th Int. Conf. on Calorimetry in High Energy Physics, La Biodola (Is. d'Elba), Italy, Sept. 20–25 1993, eds. A. Menzione and A. Scribano (World Scientific) p. 503.
[9] Ref. [3], 34.
[10] E.J. Fenyves et al., Phys. Rev D 37 (3) (1988) 649.
[11] B. D'Ettorre and G. Di Sciascio. Astron. Phys. (2) (1994) 199.
[12] Messel and Crawford, Electron-Photon Shower Distribution Functions (Pergamon, London, 1970).
[13] A. Trzupek et al., J. Phys. G. 18 (1992) 1849.
[14] K. Greisen, Progress in Cosmic Ray Physics, Vol. 3 (North-Holland, Amsterdam, 1956).
[15] W.T. Eadie, D. Drijard, F.E. James, M. Roos and B. Saodulet, Statistical Methods in Experimental Physics, (North Holland, Amsterdam and London, 1971).